Sound absorption by acoustic microlattice with optimized pore configuration

Xiaobing Cai, Jun Yang, Gengkai Hu, and Tianjian Lu

ARTICLES YOU MAY BE INTERESTED IN

Composite honeycomb metasurface panel for broadband sound absorption
The Journal of the Acoustical Society of America **144**, EL255 (2018); https://doi.org/10.1121/1.5055847

Prediction of sound absorption based on specific airflow resistance and air permeability of textiles
The Journal of the Acoustical Society of America **144**, EL100 (2018); https://doi.org/10.1121/1.5049708

Subwavelength and quasi-perfect underwater sound absorber for multiple and broad frequency bands
The Journal of the Acoustical Society of America **144**, 648 (2018); https://doi.org/10.1121/1.5048797

Effects of age and duration of deafness on Mandarin speech understanding in competing speech by normal-hearing and cochlear implant children
The Journal of the Acoustical Society of America **144**, EL131 (2018); https://doi.org/10.1121/1.5051051

Numerical observation of secondary Mach stem in weak acoustic shock reflection
The Journal of the Acoustical Society of America **144**, EL125 (2018); https://doi.org/10.1121/1.5050667

Influence of classroom acoustics on the reading speed: A case study on Italian second-graders
The Journal of the Acoustical Society of America **144**, EL144 (2018); https://doi.org/10.1121/1.5051050

Sound absorption by acoustic microlattice with optimized pore configuration

Xiaobing Cai and Jun Yang[a]

Department of Mechanical and Materials Engineering, The University of Western Ontario,
London, Ontario N6A 5B9, Canada
caixiaobing11@gmail.com, jyang@eng.uwo.ca

Gengkai Hu

School of Aerospace Engineering, Beijing Institute of Technology, Beijing 100081,
People's Republic of China
hugeng@bit.edu.cn

Tianjian Lu

State Key Laboratory for Strength and Vibration of Mechanical Structures,
Xi'an Jiaotong University, Xi'an, Shanxi 710049, People's Republic of China
tjlu@xjtu.edu.cn

Abstract: The great progress in material science and nano-micro fabrication enables the applications of metamaterials with well-defined and well-organized microstructures for noise reduction. However, what intrinsic morphology of the metamaterial would result in optimum sound absorbing efficiency remains uncertain. This work presents a microlattice metamaterial, comprising well-defined and organized material morphology in terms of pore size and porosity, for generating optimum sound dissipation. A compact governing equation is established and verified experimentally to show that the optimum sound absorption can only be reached when the pore size equals twice the thickness of a viscous boundary layer.
© 2018 Acoustical Society of America
[S-KL]
Date Received: May 16, 2018   **Date Accepted:** August 9, 2018

1. Introduction

Currently prevalent sound absorbing materials (SAMs) are featured as comprising a massive amount of intricate and interlocked irregular pores, through which sound energy is dissipated as a result of friction between the acoustic airflow and their rigid skeletons, or of thermal loss.[1–8] One limitation associated with the SAMs is that their pores are poorly controllable in both dimension and configuration. This makes the optimization on intrinsic structures of the SAMs targeting maximum sound absorptivity a challenging task, and also makes previous efforts to prefer to use flow resistance as the intermediate variable, instead of the material morphology, in SAM optimization.[8] Recently, metamaterials or metasurfaces[9–12] based SAMs providing manageable and adaptable performance are attracting growing interest; some may provide dark acoustic effect at low frequency[11] or ultra-broadband acoustic absorption.[12] These SAMs possess well-defined and organized microstructures. Nevertheless, a question still exists as to what pore size and porosity would render a SAM with maximum sound absorbing efficiency, while the existence of such an optimum pore size may be implicitly indicated.[8]

In this work, starting with a three-dimensional (3D) printed microlattice metamaterial composed of well-defined and organized micro-structures, we tailor the inner pores to be uniformly sized as twice the thickness of a viscous boundary layer of acoustic airflow. We show that this gives rise to critical friction between the airflow and the interstitial surfaces of the SAM, allowing the pore cross-sections to be completely filled up with a useful dissipative layer but concurrently to avoid over-resistance. For any given thickness, the resulting metamaterial demonstrates maximum sound absorbing efficiency, outperforming the widely recognized good sound absorber, glass fiber.[3,4] Thermo-viscous acoustic simulations on the sound absorptions are in good agreement with the experiments. In particular, a brief explicit equation regarding the optimum

---

[a]Author to whom correspondence should be addressed.

pore size is established, for which may be surprising is that it simply involves two variables, i.e., the frequency of sound and the viscosity of air.

2. Theoretical model

The proposed microlattice material is constructed of multiple layers of perforated plates, spaced apart from each other with air gaps and interconnected by micro-sized rods. As shown in Fig. 1, each monolayer of the plates is formed by micro-ridges and wires, defining uniform sub-millimeter square pores. The rods and ridges, thicker and wider than the wires, act as a solid and sturdy framework of the microlattice. Samples are prepared in a circular disk, with each sample having a peripheral wrapper layer. The morphological features of the microlattice can be precisely controlled by tuning the following parameters: pore width a, wire width w, ridge width s, square rod width W, layer thickness t, and layer spacing h.

For a perforated plate, the general form of its acoustic impedance can be expressed[6] as $z = \kappa + j\chi$, where $\kappa = (32\mu t)k_r/(\sigma\rho_0 c_0 d^2)$, $\chi = (\omega t)k_m/(\sigma c_0)$, $j^2 = -1$, t is the layer thickness, c_0 is the sound speed in air, μ is the dynamic viscosity of air, σ is the porosity, and k_r and k_m are the two variables dependent on pore diameter d. The first term κ denotes resistance and relates to the part of energy dissipation, while the second term χ denotes "reactance," and can be compensated by the distance between the plate and a rigid back wall. This could result in a maximum sound absorption coefficient in the form of $\alpha = 4\kappa/(1 + \kappa)^2$.[6] Particularly, $\kappa = 1$ results in unity absorption, i.e., $\alpha = 1$. This yields $\sigma d^2 = (32\mu t)k_r/(\rho_0 c_0)$, which can be further reduced to optimum pore radius: $r = \hat{k}\sqrt{2\mu/(\omega\rho_0)}$, with $\hat{k} = \sqrt{8\pi k_r t f/(\sigma c_0)}$ and f being the sound frequency.

Because $\hat{k}$ has a complicated form, it is important to find its value in order to determine the optimum pore radius corresponding to unity absorption. First, in our case, using the expression in Ref. 6, k_r is estimated to be around 1.0–1.2.[6] Second, after determining the frequency f and porosity σ corresponding to maximum sound
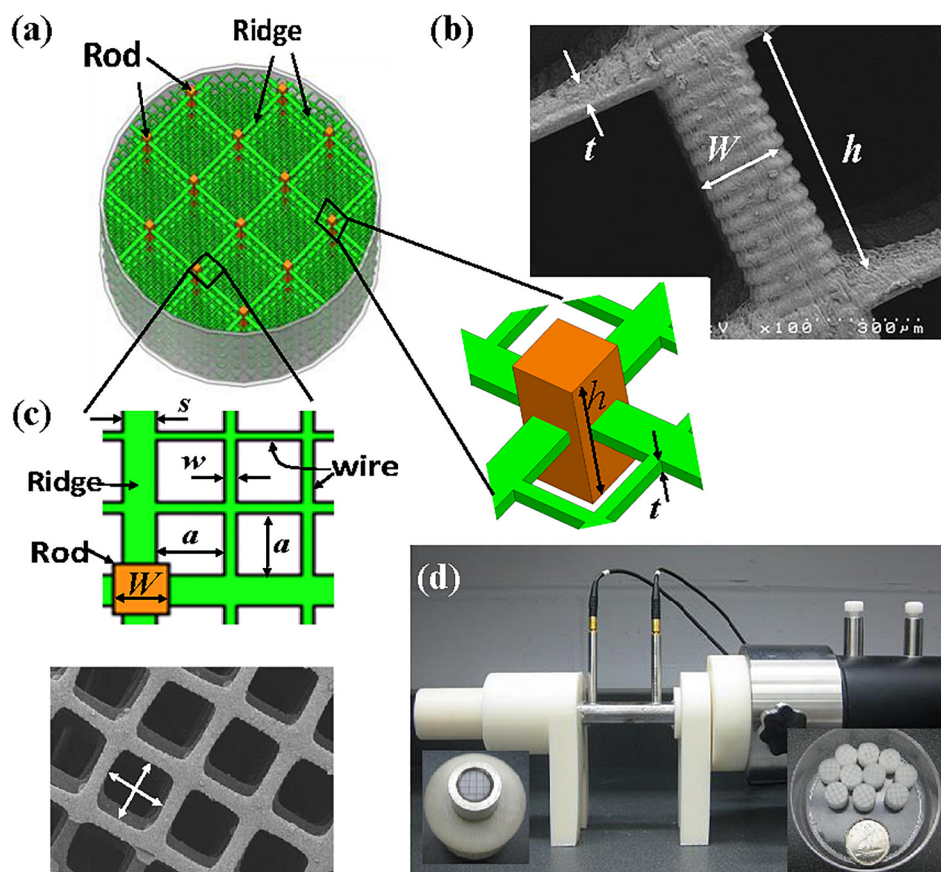
Fig. 1. (Color online) The sample of the microlattice metamaterial: (a) The microstructure of the microlattice metamaterial, (b) SEM picture of longitudinal sectional view on solid frameworks, (c) cross-section of one layer with uniformly-sized pores, and (d) the sound absorption measuring device with a modified loading portion, and ten disk-shaped samples to be tested.

absorption, it is found that f is in linear relation to σ, so that the ratio of f/σ is generally non-variable. Figure 2(a) shows the sound absorptions as functions of d and σ for twelve 1/3 octave frequencies. It is seen that porosities corresponding to maximum absorption regions increase as frequencies tone up, for which the values of f/σ for different samples can be found numerically. In addition, because each layer of the perforated plates has the same characteristic impedance and wavenumber, the thickness t now should denote the total thickness of the samples. With the ratio of f/σ and the value of t obtained, the value of $\hat{k}$ can be determined and is shown in Fig. 2(b). It may be surprising to find that its value is generally close to 1.0 ($\hat{k} = 1.0 \pm 0.07$), regardless of sample thickness t or frequency. The calculation of sound absorptivity of the microlattice is carried out by using an integrated transfer matrix method.[13] First, the complex acoustic wave number k_n and impedance z_n of the nth monolayer of the membranes are obtained using the simulated acoustic response in COMSOL Acoustics. It follows that a transfer matrix $[t_n]$ can be established to link the acoustic pressure and velocity fields at opposite sides of this layer: $[p_{n+1} u_{n+1}] = [t_n][p_n u_n]$. And then an overall transfer matrix for the whole sample can be established as $[T] = [t_1][t_2] \cdots [t_n] \cdots [t_N]$, with N being the total number of layers. As a result, the sound absorption coefficient can be calculated by using $\alpha = 1 - |R|^2$, where R is the reflectance, $R = (T_{11} - z_0 T_{21})/(T_{11} + z_0 T_{21})$, and z_0 is the characteristic impedance of air. The size of square pores investigated is between 0.05 and 0.5 mm (for circular pore $d = 2a/\sqrt{\pi}$: 0.056–0.56 mm), and the porosity is between 0.1 and 0.8. The thickness of each layer is chosen as 50 μm, while the spacing h is selected as 450 μm. Consequently, for $N = 100$, the overall sample thickness is 50 mm.

Therefore, the optimum pore radius can be rewritten as

$$r_{Opt} \approx \sqrt{2\mu/(\omega\rho_0)}, \tag{1}$$

which equals exactly the thickness of the viscous boundary layer $t_v = \sqrt{2\mu/(\omega\rho_0)}$.[2,14] Other approaches may also eventually come to a certain form of equation for optimum pore radius, such as the Johnson–Allard model,[1] or the Ingard model,[8] but such an explicit and straightforward brief form as Eq. (1) remains not reported, as to the best of our knowledge.

By satisfying Eq. (1), the acoustic airflow undergoes critical friction within the pores. The effect of the viscous boundary layer on sound wave includes permeability and dissipativity. Acoustic air medium becomes less resistant and less dissipative when it is distant from the solid-air interface. The viscous boundary layer *per se* implies a range only within which the viscosity takes effect.[14] Therefore, inside a pore, from its peripheral wall toward its center, both the resistance and dissipativity gradually decrease. If $r > t_v$, there exists a center region beyond the range of the boundary layer, so this center region is to some extent wasteful in the sense of dissipation. In contrast, if $r < t_v$, the boundary layer overlaps in the center region and results in over-resistance, making this region less penetrable, i.e., more reflective, a factor unfavorable for sound absorption. As a result, it is easy to infer that if an optimum state does exist, it should be $r = t_v$. Only under this condition, the viscous layer exactly fills up the
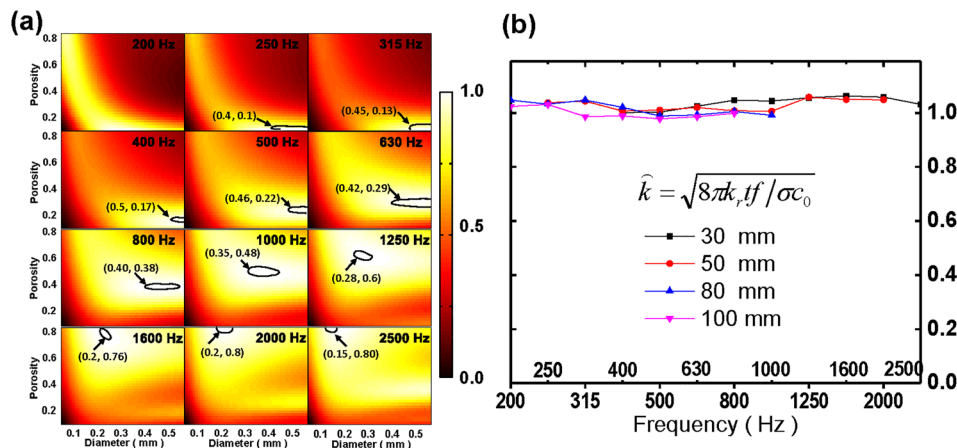
Fig. 2. (Color online) (a) The mapping of sound absorption coefficients of 50 mm thick microlattice under different pore size and porosity for 12 octave frequencies, enclosed areas indicate maximum absorption regions. (b) The numerically calculated values of $\hat{k}$ corresponding to maximum sound absorption as a function of frequency for different sample thicknesses.

pore, neither overlapping nor leaving any vacancy. Consequently, all acoustic airflow passes through the pore critically, undergoing full dissipation and concurrently experiencing the lowest reflection.

Figure 2(a) and Eq. (1) briefly reveal optimum pore size at specific frequencies, which can be readily extended to a more universal one over a wide frequency band. Further, rewriting Eq. (1) as $r_{Opt}^2 = \nu/(\pi f)$, with $\nu = \mu/\rho_0$ being the momentum diffusivity, it comes to

$$S_{Opt} = \nu T, \tag{2}$$

where $S_{Opt} = \pi r_{Opt}^2$ is the optimum cross-section area and $T = 1/f$ is the cycle. Equation (2) may be interpreted as: the optimum pore should be configured to allow acoustic airflow momentum to diffuse over its entire area within a sound cycle. Again, to the best of our knowledge, this extraordinarily brief equation has never been reported before. Since ν is typically constant, the cycle time T becomes the only parameter determining the diffusion effect of acoustic airflow. So for a noise comprising a series of frequencies f_i or cycles $T_i = 1/f_i$, each corresponding to an area $S_{Opt,i} = \nu T_i$, the total area needed for all momentum diffusion would be obtained as $S = \sum_I \nu T = \sum_I S_{Opt,i}$, with I the total number of frequencies in consideration. On average, the amount of momentum diffusion over all the frequencies is $\bar{S} = S/I = \sum_I S_{Opt,i}/I$. If such a sum of diffusion arises from a single pore, it should be sized as: $\bar{r} = \sqrt{\bar{S}/\pi}$.

The resulting universal optimum pore size can be verified from the overall rating of the microlattice material. One widely used rating of sound absorption is the Sound Absorption Average (α_{SAA}),[15] which uses the average of sound absorption coefficients from twelve 1/3 octave frequencies. Figure 3(a) shows the SAA mapping of the microlattice over pore size and porosity. A region of remarkable maximum α_{SAA} (0.72) can be seen at a pore size (diameter) around $180\,\mu m$ ($r_{Opt} = 90\mu m$) and a porosity above 0.56. The calculated optimum radius using $\bar{r} = \sqrt{\sum_I r_i^2/I}$ is around $95\,\mu m$, which is in excellent agreement with that derived from Fig. 3(a). In Fig. 3(a), a dashed line indicating a universal optimum combination of pore size and porosity is also shown. An expression of this curve is found to be $\sigma d^2 = \breve{c}_2 k_r$, according to data fitting, with $\breve{c}_2$ a constant simply determined by using initial values: $\breve{c}_2 = 0.56 * 0.18^2$. This expression is a reduction of $\sigma d^2 = (32\mu t)k_r/(\rho_0 c_0)$, by defining $\breve{c}_2 = (32\mu t)/(\rho_0 c_0)$ and by using $k_r = 1.0$, as discussed previously. Figure 3(b) shows the required thickness for reaching a target SAA = 0.7, in which a corresponding region denoting minimum thickness of 50 mm can be seen. This also confirms that the predicted optimum pore size and matched porosity offer the most efficient sound absorption.

3. Experiment and results

For experimental verification, the diameter of the pores of the microlattice materials can be chosen between $d = 180$ and $d = 220\,\mu m$, or equivalently for square pores, between $a = 160\,\mu m$ and $a = 195\,\mu m$. Without losing importance, the actual pore width is selected as integer multiple times of $39\,\mu m$, which is the XY in-plane resolution of
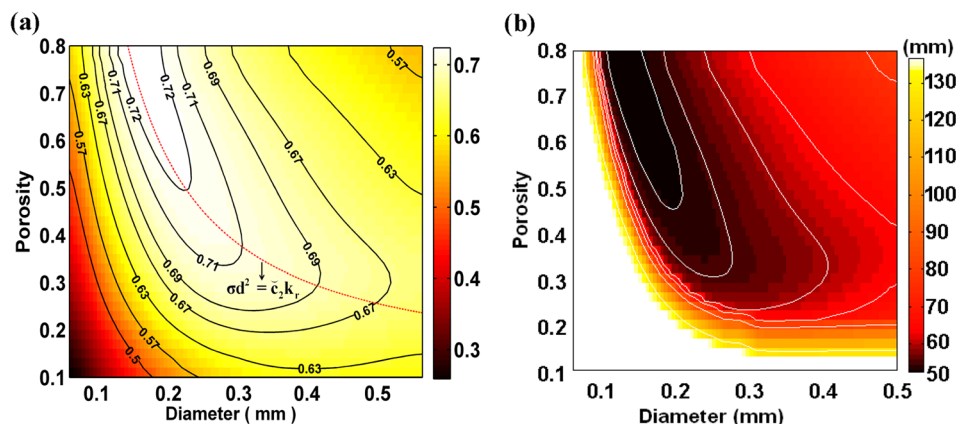
Fig. 3. (Color online) (a) The distribution SAA over 12 octave frequencies of microlattice of 50 mm thickness, maximum sound absorption region locates at pore size of $180\,\mu m$ and porosity above 0.56. (b) The required sample thicknesses for achieving a target SAA 0.7 under different pore size and porosity, minimum required thickness region exists at the similar location as that in (a).

the adopted Asiga Pico 2-39 3D printer. So, the pore width is finally chosen as $a = 195\,\mu m$ (i.e., $d = 224\,\mu m$). Another microlattice sample having a larger pore width $a = 468\,\mu m$ (i.e., $d = 528\,\mu m$) and $\sigma = 0.56$ was also fabricated for comparison. The cross-sectional planes of each microlattice sample were directly modeled in a digital matrix, with each element of the microlattice encoded into pixels, denoted by either 1 or 0 in the matrix. During printing, the exposure time for the photosensitive polymer and other machine parameters were carefully adjusted. Upon completion, the printed sample was transferred from the printer's building platform into ethyl alcohol for ultrasonic treatment for 30 s to remove the adhering uncured resin.

As shown in Fig. 1(c), the samples have uniformly sized pores that are formed by micro wires. Pores with uniform width $a = 190\,\mu m$ (slightly smaller than the designed value of 195 μm) and wires of 45 μm can be seen [Fig. 1(c)]. Accounting for all the solid parts, i.e., the rods, wires, and peripheral wrapper layer, the actual in-plane porosity is 56%. Scanning electron microscope (SEM) images offer details of the layers and rods [Figs. 1(b) and 1(c)], showing excellent structural control in microfabrication, with seamless bonds intermediating rods and ridges that constitutes a solid and stable framework. Taking the space between two adjacent layers into account, the volumetric porosity (σ_V) is estimated as high as 94%, resulting in small interlayer airflow resistance that ensures an impedance match between incident air medium and the bulk sample.

To experimentally characterize the sound absorbing efficiency of these 3D-printed microlattice materials, bulk samples were prepared as circular disks [Fig. 1(d)] with a diameter of 9.84 mm and a height of 5 mm (i.e., 10 layers of membranes). A stack of 10 disks (total thickness $H = 50$ mm) was mounted into a sound impedance tube having the same inner diameter ($D = 9.84$ mm), backed by a rigid steel plate of thickness 5 mm (not shown). This impedance tube is a holder of a standard sound absorption coefficient measuring device [Fig. 1(d)].

The measured sound absorption properties of the microlattice samples are shown in Fig. 4(a). Good agreement between experimental (dashed lines) and numerical (straight line with scatters) results can be seen. The microlattice material samples with optimum pore configuration show enhanced performance among all the frequencies. The performance of the present microlattice materials having optimum structures is compared with that of common SAMs, shown in Fig. 4(b). It can be noted that the optimized microlattice ($a = 190\,\mu m$, $\rho = 66\,mg/cm^3$, $\sigma_V = 0.94$) outperforms the glass fiber ($\rho = 32\,mg/cm^3$, $\sigma_V = 0.98$) (dashed line) throughout all frequencies, while the latter is widely recognized as a good absorber when proper density and porosity are selected.[3,4] Other popularly used sound absorbers, such as foams, are generally 0.3–0.4 underperforming than the microlattice. It is also worth noting that the 3D printed microlattice is a solid structure with inherent high stiffness/mass ratio, which provides it with greatly improved stability and reliability. The significant enhancement in absorptivity of microlattice with optimum microstructures signifies a new avenue for design and manufacturing of next generation SAMs.

4. Conclusion

Through theoretical analysis, numerical and experimental investigation on sound absorption by microlattice material with well-defined microstructures, it is found that
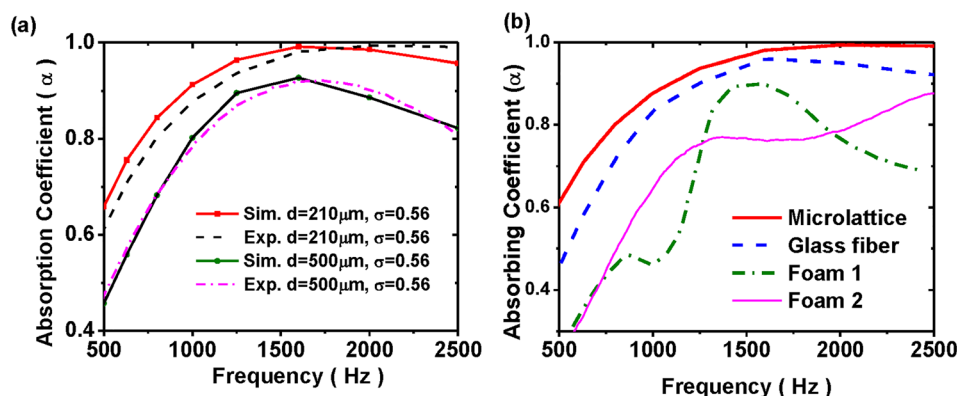
Fig. 4. (Color online) Sound absorbing properties of microlattice materials. (a) Numerical and experimental results of sound absorbing coefficient agree with each other for microlattice samples with width $a = 190\,\mu m$ (i.e., $d \approx 210\,\mu m$) and $a = 468\,\mu m$ (i.e., $d \approx 500\,\mu m$). (b) Comparison of absorbing coefficients between the microlattice materials and other SAMs.

the optimum pore size for maximum sound absorption is twice the viscous boundary layer thickness. This surprisingly brief relation was not explicitly presented before, as to the best of our knowledge. In addition, optimum combinations of pore size and porosity for maximal sound absorption over the entire frequency band were also determined for practical applications. The findings in this work offer a useful guide for designing SAMs with enhanced performance.

Acknowledgments

References and links

[1] J. F. Allard and Y. Champoux, "New empirical equations for sound propagation in rigid frame fibrous materials," J. Acoust. Soc. Am. **91**, 3346–3353 (1992).

[2] M. R. Stinson, "The propagation of plane sound waves in narrow and wide circular tubes, and generalization to uniform tubes of arbitrary cross-sectional shape," J. Acoust. Soc. Am. **89**, 550–558 (1991).

[3] Y. Yang, B. Li, Z. Chen, N. Sui, Z. Chen, T. Xu, Y. Li, R. Fu, and Y. Jing, "Sound insulation of multilayer glass-fiber felts: Role of morphology," Text. Res. J. **87**, 261–269 (2017).

[4] M. E. Delany and E. N. Bazley, "Acoustical properties of fibrous absorbent materials," Appl. Acoust. **3**, 105–116 (1970).

[5] E. Blanc, G. Chiavassa, and B. Lombard, "Time-domain numerical modeling of two-dimensional wave propagation in porous media with frequency-dependent dynamic permeability," J. Acoust. Soc. Am. **134**, 4610–4623 (2013).

[6] D. Maa, "Potential of microperforated panel absorber," J. Acoust. Soc. Am. **104**, 2861–2866 (1998).

[7] M. Hakamada, T. Kuromura, Y. Chen, H. Kusuda, and M. Mabuchi, "High sound absorption of porous aluminum fabricated by spacer method," Appl. Phys. Lett. **88**, 254106 (2006).

[8] K. U. Ingard, *Notes on Sound Absorption Technology* (Noise Control Foundation, New York, 1994).

[9] M. Yang, S. Chen, C. Fu, and P. Sheng, "Optimal sound-absorbing structures," Mater. Horiz. **4**, 673–680 (2017).

[10] M. Yang and P. Sheng, "Sound absorption structures: From porous media to acoustic metamaterials," Ann. Rev. Mater. Res. **47**, 83–114 (2017).

[11] J. Mei, G. Ma, M. Yang, Z. Yang, W. Wen, and P. Sheng, "Dark acoustic metamaterials as super absorbers for low-frequency sound," Nat. Commun. **3**, 756 (2012).

[12] X. Jiang, B. Liang, R. Li, X. Zou, L. Yin, and J. Cheng, "Ultra-broadband absorption by acoustic metamaterials," Appl. Phys. Lett. **105**, 243505 (2014).

[13] X. Cai, J. Yang, and G. Hu, "Optimization on microlattice materials for sound absorption by an integrated transfer matrix method," J. Acoust. Soc. Am. **137**, EL334–EL339 (2015).

[14] G. Kirchhoff, "Ueber den einfluss der wärmeleitung in einem gase auf die schallbewegung," Ann. Phys. (Berlin) **210**, 177–193 (1868).

[15] ASTM C423-09a, Standard Test Method for Sound Absorption and Sound Absorption Coefficients by the Reverberation Room Method (ASTM, West Conshohocken, 2009).